Comparison of Structure and Properties of Conventional and "High Crystallinity" Isotactic Polypropylenes and Their Blends with Metallocene-Catalyzed Linear Low Density Polyethylene. II. Morphological Studies

N. KUKALEVA,[1,2] F. CSER,[2] M. JOLLANDS,[1] E. KOSIOR[3]

[1] Royal Melbourne Institute of Technology (RMIT), Department of Chemical and Metallurgical Engineering, GPO Box 2476v, Melbourne, 3001, Australia

[2] Cooperative Research Centre for Polymers, Notting Hill, Victoria, 3168, Australia

[3] Visy Plastics, 268 Edwardes Street, Reservoir, Victoria, 3073, Australia

Received 8 September 1999; accepted 17 March 2000

ABSTRACT: The morphology of "high crystallinity" polypropylene (h.cr.PP) and metallocene-catalyzed linear low density polyethylene blends has been investigated using optical microscopy, scanning electron microscopy, and wide-angle X-ray scattering. The data obtained were analyzed and compared with results from physical testing. It was concluded that the improved physical performance of pure h.cr.PP, as well as its blends, compared with conventional PP and its blends was due to the alteration (suppression) of spherulitic structure of the former caused by the presence of nucleating agents. These additives (nucleating agents) appear also to cause the formation of fine lamellae in h.cr.PP, which could be an additional factor contributing to the improvement of the properties. A co-continuous structure of the blends comprised from two phases is shown to be superior to a matrix-dispersed one for improving the balance of mechanical properties. Co-continuity can exist and contribute to the improvement of the properties in systems either with or without spherulites. © 2001 John Wiley & Sons, Inc. J Appl Polym Sci 80: 831–840, 2001

Key words: polypropylene; spherulitic structure; co-continuity; polymer blends

INTRODUCTION

In this study, we investigate the reasons for the improvements in physical properties for a so-called "high crystallinity" polypropylene (PP) compared with a conventional PP. In Part I, relations between rheological behavior and thermal and physical properties were analyzed.[1] In this second part, the morphological studies are performed. The structure-property relationships of the "high crystallinity" PP and metallocene-catalyzed linear low density polyethylene blends are examined to verify the applicability of the conclusion made previously[2] about the superiority of a co-continuous structure compared with a matrix-dispersed one for blends of conventional PP and

Correspondence to: N. Kukaleva (natalia.kukaleva@eng.monash.edu.au).

Contract grant sponsors: Royal Melbourne Institute of Technology and Cooperative Research Centre for Polymers.

Journal of Applied Polymer Science, Vol. 80, 831–840 (2001)

metallocene-catalyzed linear low density polyethylene.

EXPERIMENTAL

Materials

The same types of isotactic PP homopolymers as specified in Part I were used: the "high crystallinity" PP (h.cr.PP)—K2XMOD with melt flow index (MFI) = 8 [g/10 min] (2.16 kg, 230°), supplied by PCD Polymere, Austria, and a conventional grade of PP (conv.PP)—GWM 22 with MFI = 4 [g/10 min] (2.16 kg, 230°), supplied by ICI, Australia. These two PPs were blended with a grade of metallocene-catalyzed ethylene-octene copolymer ENGAGE EG 8200 with MFI = 5 [g/10 min] (2.16 kg, 190°C), referred to as mLLDPE. ENGAGE EG 8200 was supplied by Dow Plastics, Australia.

Blends and Samples Preparation

Blends of PP/mLLDPE (90:10, 80:20, 70:30, 60:40, 50:50, and 40:60) were prepared by extrusion and test samples were produced by injection molding. The setup was identical to that specified elsewhere.[2]

Morphological Characterization

Optical Microscopy (OM)

Samples were cut from injection-molded tensile test samples: 1. bars with width about 5 mm were cut from the narrow section of the tensile test pieces perpendicular to the direction of the long axis; 2. thin sections (1–5 μm) were cut perpendicular to the width of these bars.

For pure PPs and compositions 90:10, 80:20, 70:30, 60:40, and 50:50 PP/mLLDPE the sections were obtained by a Reichert Ultracut 3 Ultramicrotome using a 45° glass knife at room temperature, producing sections of 5 μm. For pure mLLDPE and compositions of 40:60 PP/mLLDPE, sections were cut by the same type of knife at −120°C in an FCS (liquid nitrogen operated) cooling device attached to the Ultramicrotome. The change in the cutting temperature was required because 40:60 compositions, as well as pure mLLDPE, were too soft and "viscous" to be cut at room temperature. One micron was the maximal thickness of the sections that could be obtained from the "frozen" samples.

An Olympus BX60 F-3 polarizing microscope was used to obtain optical micrographs. Two magnifications were applied using DPlan 4PO (0.1) 160:0.17 and MPlan 40:0.40 SLWD objectives. This made an overall magnification of ×135 and ×680 on a 9 × 14 cm sheet paper (photographs were made using a 5.3 projector).

Because of limited space, the photographs with low magnification are not presented in this article but are available upon request.

Scanning Electron Microscopy (SEM)

Two types of fracture surfaces were studied with a JEOL JSM 840 A scanning electron microscope. Impact test bars of the compositions to be examined were immersed in liquid nitrogen for 10 min, followed by mechanical fracture. The second type of surface of samples was obtained for examination when the test specimen was fractured in Izod impact tests at room temperature.

The samples were coated with gold using a DYNAVAC sputter coater. The periods of applying voltage (5 s) alternated with pauses of similar length. The number of coating cycles (voltage-pause) was forty.

X-ray Diffraction

A Rigaku Geigerflex generator with a DMAXB controller was used for a wide angle X-ray scattering (WAXS) study. A 30-kV accelerating voltage and a 30-mA current were applied using Ni-filtered Cu-Kα radiation. WAXS intensities were recorded from $2\Theta = 3°$ to $2\Theta = 50°$ in transmission mode on injection-molded samples (tensile test bars) with a 3-mm thickness. A continuous scan of $\Delta 2\Theta = 2°$/min with data collection at each 0.05° of 2Θ was performed.

RESULTS AND DISCUSSION

Optical Microscopy

Microtomed sections of the blends and the blends' components were viewed in crossed polarized light. The spherulitic morphology of conv.PP was observed for the range of the compositions with 100–70% of PP. The spherulite size of the PP appears to decrease consistently with an increase of the level of mLLDPE phase in a blend (sizes are recorded in Table I). Figure 1 shows polarizing optical micrographs of pure conv.PP (a), 80:20 (b), and 50:50 (c) conv.PP/mLLDPE blends.

Table I Influence of Composition on the Size of Spherulites in the Conv.PP/mLLDPE Blends

Composition	Spherulitic Size
100% conv.PP	28–30μm
90 conv.PP/10 mLLDPE	20–22μm
80 conv.PP/20 mLLDPE	15–17μm
70 conv.PP/30 mLLDPE	10–12μm

The observed trend agrees with data published by Coppolal et al.[3] and Chou et al.[4] for iPP/rubber (EPR) blends: in both of these studies the spherulites of PP gradually became smaller as the EPR content increased. The study conducted by Bartczak et al.[5] also showed a decrease in the spherulite growth rate and the size of PP spherulites in its blends with LDPE and several elastomers. A "drastic" [sic] decrease in the spherulite size of the PP in the presence of LDPE was also described by Lovinger and Williams[6] and Teh.[7]

A spherulitic structure was not observed in the conv.PP compositions with mLLDPE contents of 40% and more. This observation is consistent with the data reported by Kresge[8] and Cser et al.[9] The latter claimed that spherulitic size of PP decreased in a consistent manner with an addition of LLDPE up to 40% in the blend. For the compositions with 40% and above (50 and 60% of LLDPE), spherulites were not observed. Kresge[8] also did not find any spherulites for elastomeric blends of isotactic PP with EPR at similar concentrations of the blends' components. It is likely that this phenomenon (the apparent "disappearance" of PP spherulites in the compositions with high concentrations of the second component) is typical for polypropylene blends with any type of α-olefins. It is possible that in these compositions, PP spherulites are very small and are disguised by the mLLDPE phase.

A spherulitic morphology was not seen either in any samples of the h.cr.PP/mLLDPE blends or in the pure h.cr.PP. In other words, there was no noticeable change in the appearance of the micrographs depending on composition. This is why only the micrograph representing pure h.cr.PP is presented in this report (Fig. 2).

It appears that either the dimension of spherulites of h.cr.PP is less than 1 μm or h.cr.PP does not possess spherulitic structure at all. In either case, such morphology is probably caused by the presence of some kind of nucleating agents in h.cr.PP. It is likely that it is not the assumed "large" difference in the levels of crystallinity compared with conventional PP (only about 5%) by modulated differential scanning calorimetry (MDSC) results,[1] but this unique "non-spherulitic" structure of the former that is responsible for the improved mechanical properties described in Part I.

SEM

SEM on the Cryofractured Surfaces

A typical dispersed-matrix structure of the blends is apparent in Figure 3, representing h.cr.PP/mLLDPE compositions with 10 (a), 20 (b), and 30% (c) of mLLDPE phase, correspondingly. Particles of mLLDPE are dispersed within a matrix of h.cr.PP. Their size grows from 0.3 to 1.0 μm, their areal fraction from 3 to 7%. Figure 4 shows the cryofractured surfaces of blends with 40 (a), 50 (b), and 60% (c) of mLLDPE. For these compositions, the mLLDPE phase does not remain as distinct dispersed domains, but seems to form a continuous phase within the h.cr.PP phase. Generally, the appearance of the cryofractured surfaces of h.cr.PP/mLLDPE blends does not differ much from those of conv.PP/mLLDPE blends given in our previous report.[2]

As mentioned above, the areal fraction of the mLLDPE phase was found to be 3 to 7% for blends with 10–30% of mLLDPE. A similar "shortage" in the dispersed particles was reported for conv.PP/mLLDPE blends as well.[2] This "shortage" for the h.cr.PP/mLLDPE systems with mLLDPE content up to 30% indicates that mLLDPE is not present purely as a dispersed phase.

SEM on the Fractured Surfaces Created at Ambivalent Temperature

Blends with 10% of mLLDPE. The fracture surfaces of the compositions with 10% of mLLDPE (Fig. 5) show the dispersed-matrix type of structure similar to the cryofractured surface of the same blend [Fig. 3(a)]. If the appearance of the fractured surfaces of h.cr.PP/mLLDPE and conv.PP/mLLDPE blends[2] is compared, the amount of mLLDPE particles/holes seen on the fractured surface of the former seems to be smaller than that on the fractured surface of the conv.PP/mLLDPE blend. Another difference is that the size of the domains of the dispersed phase in the conv.PP/mLLDPE blend is very homogeneous (0.3 μm), whereas that in the h.cr.PP matrix varies between 0.3–0.6 μm.

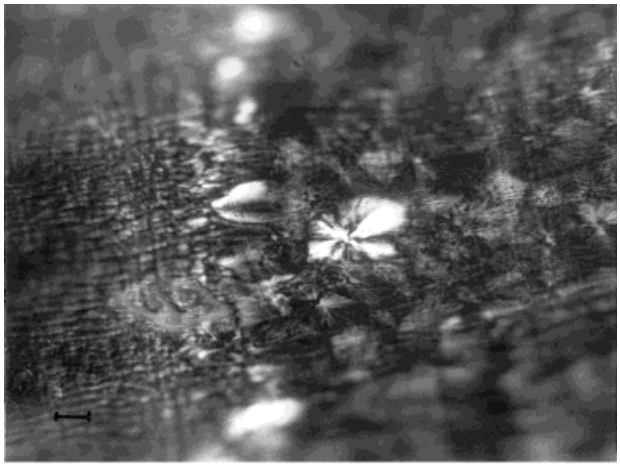

(a)

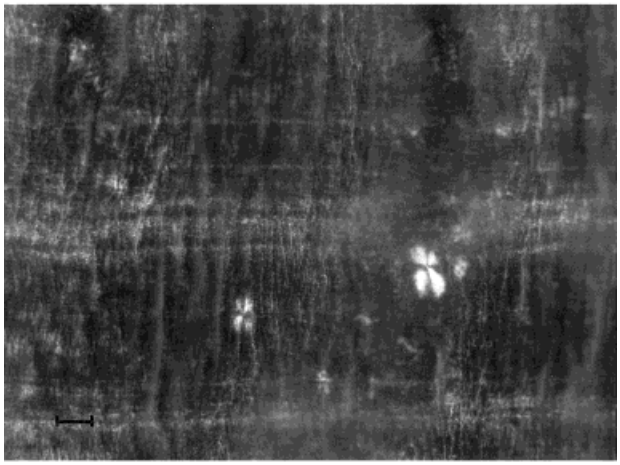

(b)

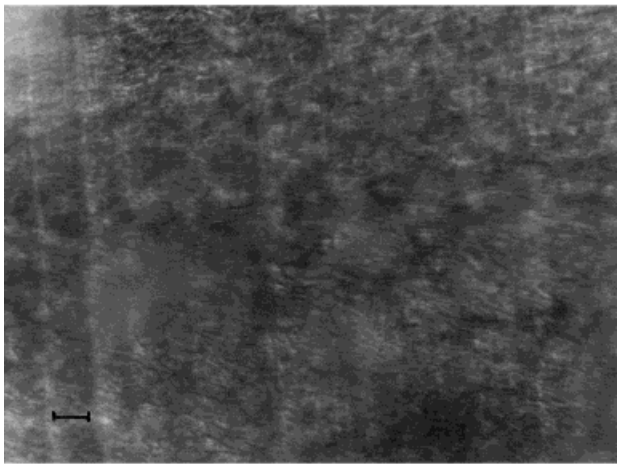

(c)

Figure 1 (a) Polarized light micrograph of conv.PP, original magnification ×680. Bar represents 10 μm. (b) Polarized light micrograph of 80 conv. PP/20 mLLDPE, original magnification ×680. Bar represents 10 μm. (c) Polarized light micrograph of 50 conv.PP/50 mLLDPE, original magnification ×680. Bar represents 10 μm.

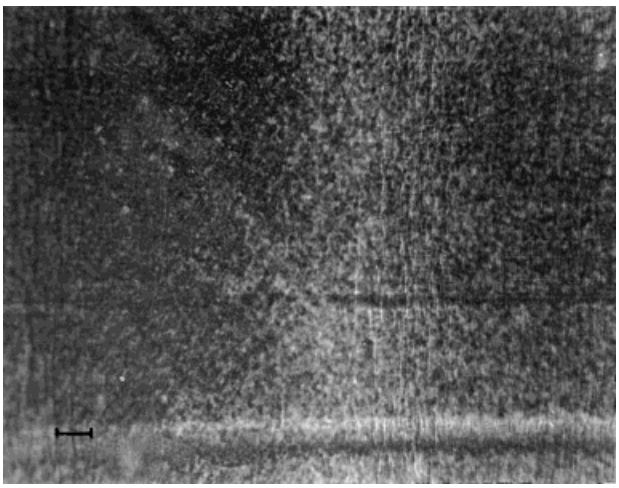

Figure 2 Polarized light micrograph of h.cr.PP, original magnification ×680. Bar represents 10 μm.

Blends with 20% of mLLDPE. The structure of 80:20 compositions differs radically for h.cr.PP and conv.PP. For the h.cr.PP blend, the appearance of the fracture surface depends on the distance from the notch. This is why two micrographs for the h.cr.PP/mLLDPE blend with 20% of mLLDPE [Fig. 6 (a,b)] were taken. Both of them differ to a great degree from the micrograph of the same blend at the same magnification of the cryofractured surface [Fig. 3(b)].

Micrograph 6(a) represents the area in the vicinity of the notch. The particles of the dispersed phase are not seen on the fracture surface shown. Examination of the places, from where they were pulled out, shows that: 1. the "particles" of the dispersed phase, and, correspondingly, the "holes" (voids) left, have lost their spherical shape; and 2. the "holes" (voids) have increased in apparent size and "depth." The size of mLLDPE inclusions was determined to be 0.5–2 μm (compare with 0.6 μm for the cryofractured surface).

From this micrograph [Fig. 6(a)], it is clear that the blend cannot be regarded as being of a traditional dispersed-matrix type due to the severe distortions of the dispersed phase observed.

The area further from the notch [Fig. 6(b)] has a well-constructed lamellae structure, and inclusions of the dispersed phase are not seen at all.

Blends with 30% of mLLDPE. An exquisite three-dimensional co-continuous lamellar structure of this blend is shown in Figure 7(a), (b) and (c). The co-continuous structure of the 70 h.cr.PP/30 mLLDPE blend, shown in Figure 7(a) and (b), looks

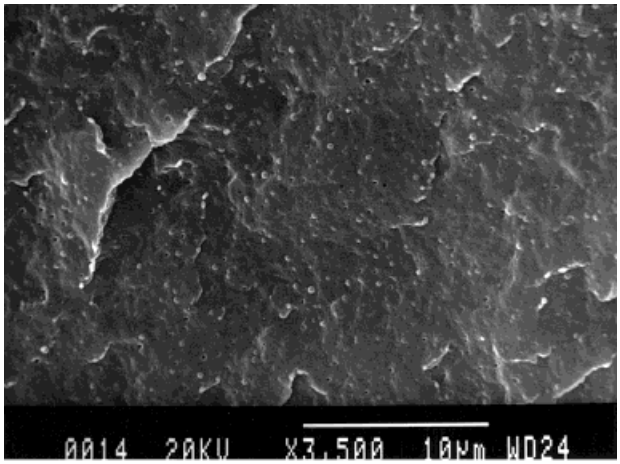

(a)

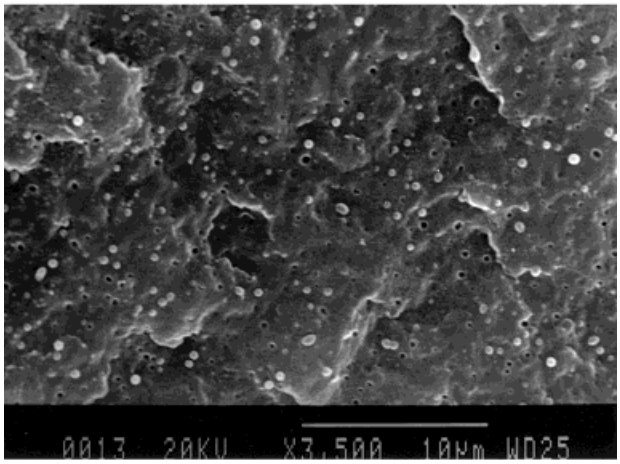

(b)

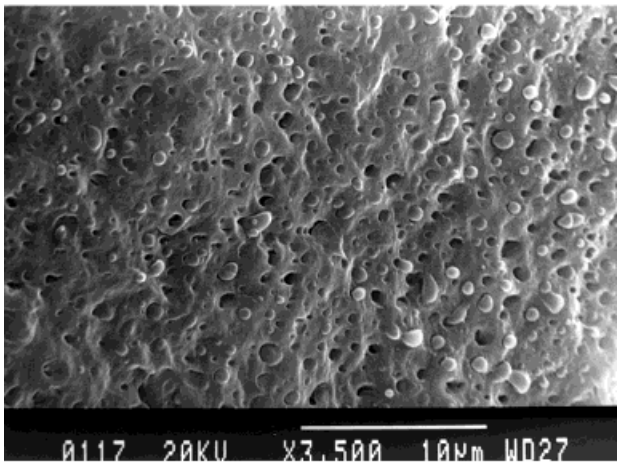

(c)

Figure 3 (a) SEM image of a cryofractured 90 h.cr.PP/10 mLLDPE specimen, original magnification ×3500. (b) SEM image of a cryofractured 80 h.cr.PP/20 mLLDPE specimen, original magnification ×3500. (c) SEM image of a cryofractured 70 h.cr.PP/30 mLLDPE specimen, original magnification ×3500.

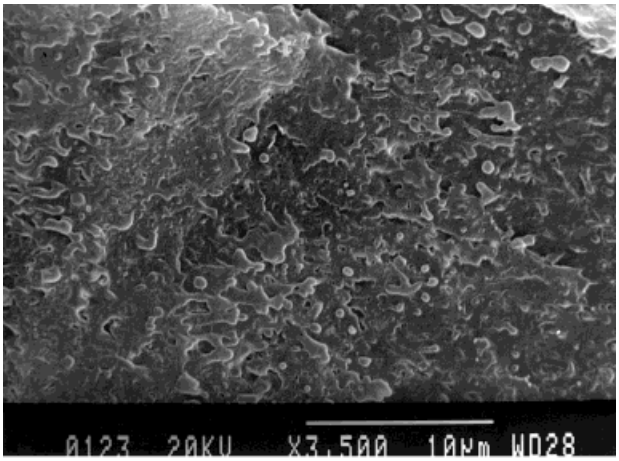

(a)

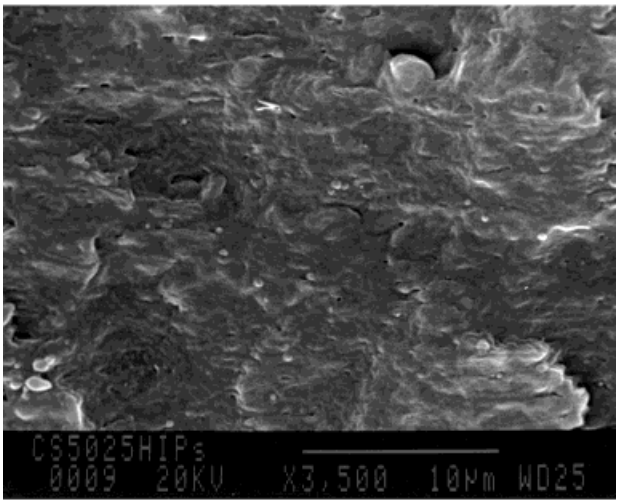

(b)

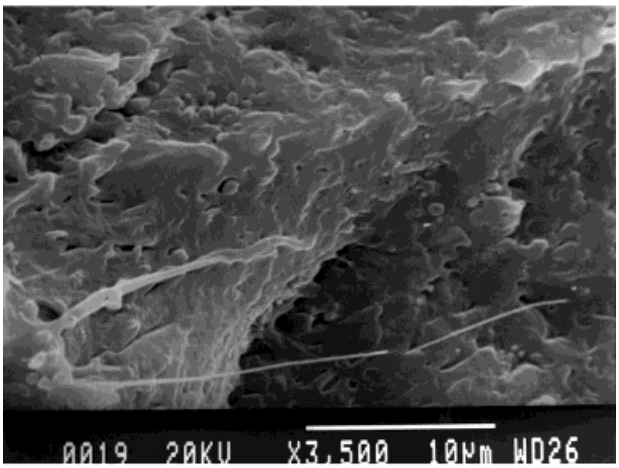

(c)

Figure 4 (a) SEM image of a cryofractured 60 h.cr.PP/40 mLLDPE specimen, original magnification ×3500. (b) SEM image of a cryofractured 50 h.cr.PP/50 mLLDPE specimen, original magnification ×3500. (c) SEM image of a cryofractured 40 h.cr.PP/60 mLLDPE specimen, original magnification ×3500.

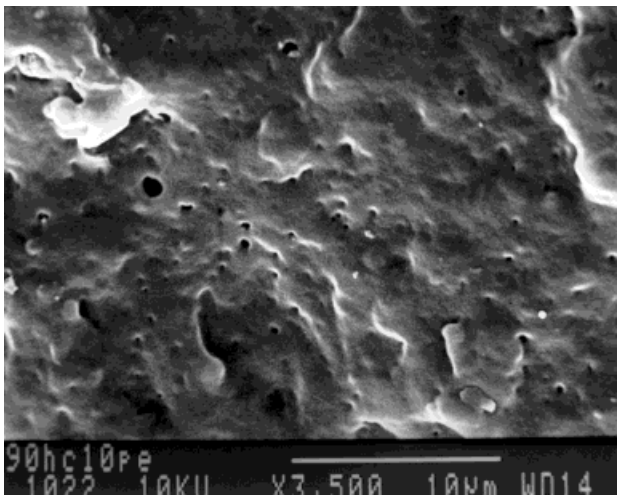

Figure 5 SEM micrograph of a fractured 90 h.cr.PP/10 mLLDPE specimen, original magnification ×3500.

like a further development of the greatly distorted dispersed-matrix structure seen in the 80:20 blend [Fig. 6(a)]. By analogy, the well-defined lamellae in Figure 7(c) appear to be a logical sequel and "growth" of lamellae shown in Figure 6(b). It seems that the morphology of the composition with 20% of mLLDPE was an intermediate between a dispersed-matrix (Fig. 5) and a co-continuous (Fig. 7) type of structure.

It is noteworthy that the dimensions of the continuous mLLDPE phase on surfaces fractured at room temperature [Fig. 7(a,b)] are much larger than the size of mLLDPE domains observed after cryofracture [Fig. 3(c)]. One of the possible reasons for this is that these blends possess a complex structure that combines dispersed-matrix and co-continuous types.

Blends with 40% of mLLDPE. The Figure 8 micrograph shows the fracture surface of the composition with 40% mLLDPE. The surface shown is characterized by multiple soft lamellae which are about 100 nm in size or below. It seems that for this composition the mode of fracture was dominated by yielding.

Overall, the outstanding physical properties for h.cr.PP/mLLDPE blends reported in Part I[1] appear to correlate with the presence of a co-continuous lamellar structure. The finer lamellae in h.cr.PP compared with conv.PP may be due to the presence of nucleating agents in composition of the former.

WAXS Study

Figure 9 represents WAXS intensities for the three blend components. The WAXS intensities for both h.cr.PP and conv.PP have a broad amorphous background superimposed on six distinct peaks at the same values of 2θ angles. These "peak" values of 2θ are 14.05°, 16.85°, 18.45°, 21.6°, 25.5°, and 28.65°. They correspond to the nominal "peak" values of α-monoclinic crystalline form of isotactic polypropylene.[10]

There is a small additional peak at 15.6° on the conv.PP curve that corresponds to the β-hexago-

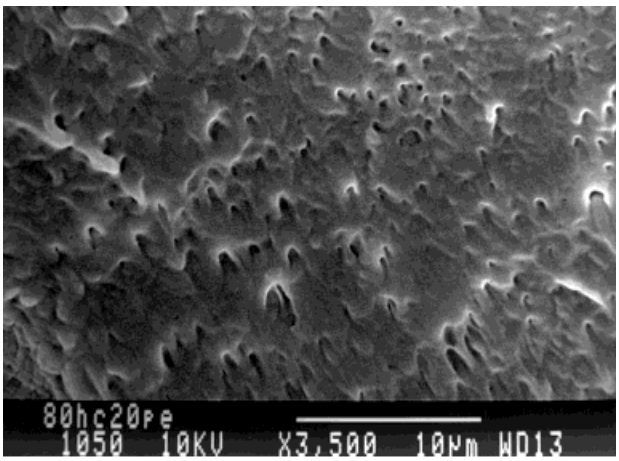

(a)

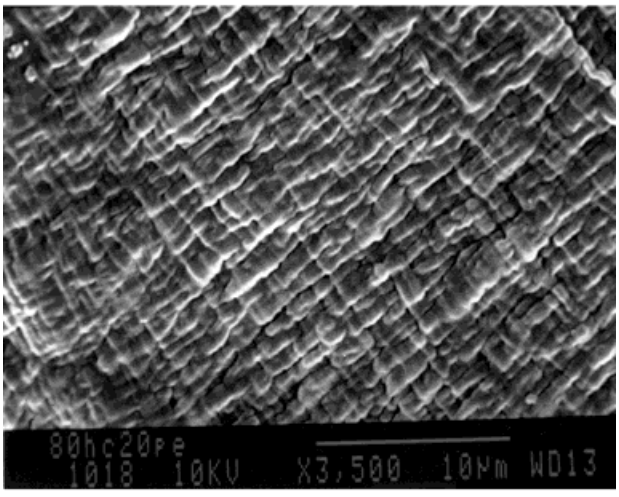

(b)

Figure 6 (a) SEM micrograph of a fractured 80 h.cr.PP/10 mLLDPE specimen, the area in vicinity of the notch, original magnification ×3500. (b) SEM micrograph of a fractured 80 h.cr.PP/10 mLLDPE specimen, the area further from the notch, original magnification ×3500.

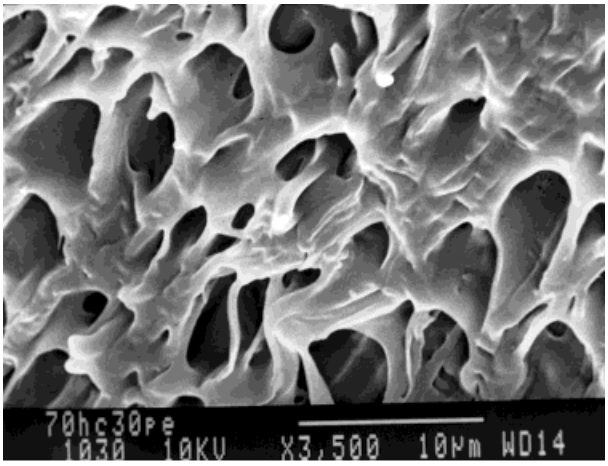

(a)

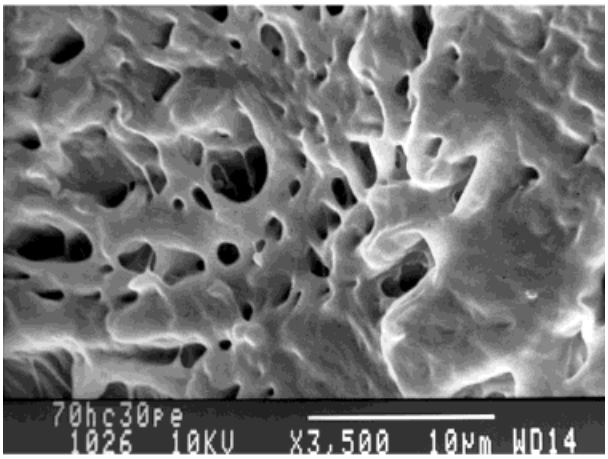

(b)

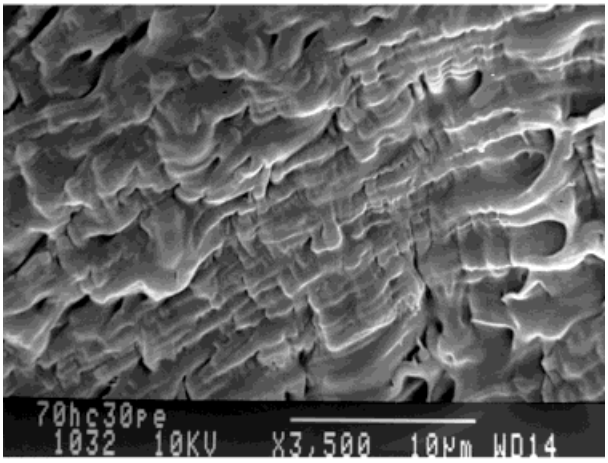

(c)

Figure 7 (a) SEM micrograph of a fractured 70 h.cr.PP/30 mLLDPE specimen, the area in vicinity of the notch, original magnification ×3500. (b) SEM micrograph of a fractured 70 h.cr.PP/30 mLLDPE specimen, the area in vicinity of the notch, original magnification ×3500. (c) SEM micrograph of a fractured 70 h.cr.PP/30 mLLDPE specimen, the area further from the notch, original magnification ×3500.

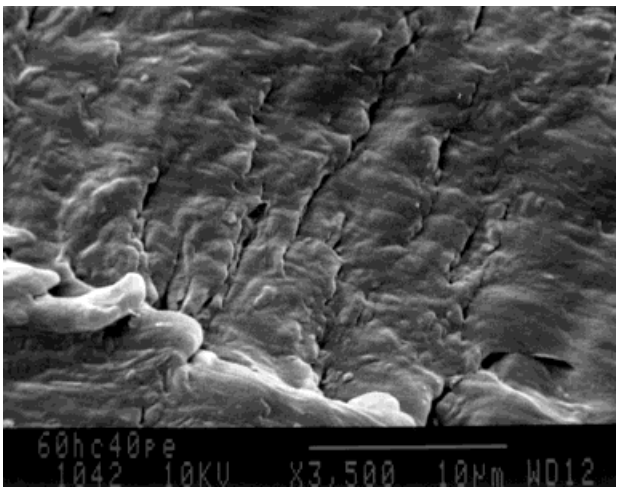

Figure 8 SEM micrograph of a fractured 60 h.cr.PP/40 mLLDPE specimen, original magnification ×3500.

nal crystalline form of polypropylene.[11] β-spherulites were also seen in optical microphotographs of conv.PP and its blends [Fig. 1(a,b)]. On the other hand, no indication of the presence of the crystalline β-form was found either by WAXS (in position of peaks) or by MDSC (in melting temperature/double melting peak[7,12]) in h.cr.PP.

The patterns of WAXS curves for the h.cr.PP and conv.PP show relatively incongruous intensities for the four peaks (at 16.85°, 18.45°, 21.6°, and 25.5°). The difference in the relative values of intensities indicates the presence of some preferred orientation of the crystals of the h.cr.PP that may have been caused by the injection-molding process. The oriented intensities of h.cr.PP appear to be entirely consistent with the proposal of its phenomenological non-spherulitic structure (see Optical Microscopy).

There is a small and broad peak at low angles (approximately at 8°) on the h.cr.PP curve that might be due to the presence of nucleating agents. If so, these are the nucleating agents that are responsible for the extremely high crystallization temperature reported in MDSC results[1] and for the "non-spherulitic," fine lamellae structure (discussed above) of h.cr.PP and its blends. Because there is a higher absorption of X-rays in the h.cr.PP compared with the conv.PP, it appears that these nucleating agents are inorganic in nature. The polymer might contain very fine mica.[13]

The WAXS curve for mLLDPE has one very broad maximum at the scattering angle 2Θ equal to 19.65°. This scattering curve is similar to

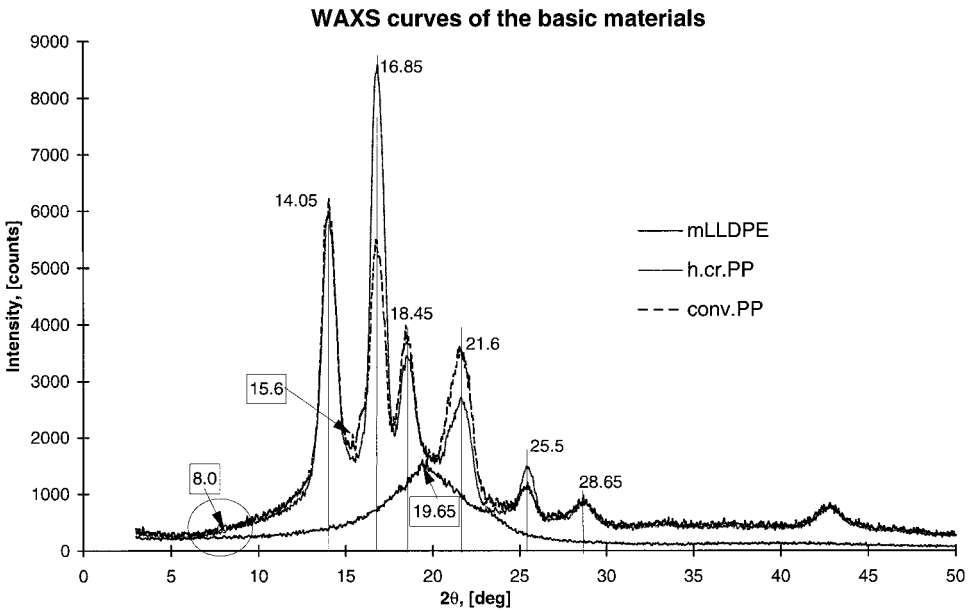

Figure 9 WAXS curves of the basic materials.

curves obtained for amorphous materials and liquids—their structure does not have periodicity and consequently does not display the sharp peaks of crystalline/semicrystalline materials. Generally, for amorphous materials, the position of the maximum corresponds to the most probable interatomic distance within the structure.[14] For the mLLDPE analyzed, the maximum on the WAXS curve corresponds to the distance (the Bragg's period) of 0.452 nm. The unsmooth appearance of this curve might be caused by a small amount of crystallinity present (1–2%) in mLLDPE.

Figures 10 and 11 show WAX scattering curves of the blends h.cr.PP and conv.PP, respectively. As expected, there is no measurable shift in the position of the neat PPs' peaks compared with the blends' peaks. It means that both h.cr.PP and

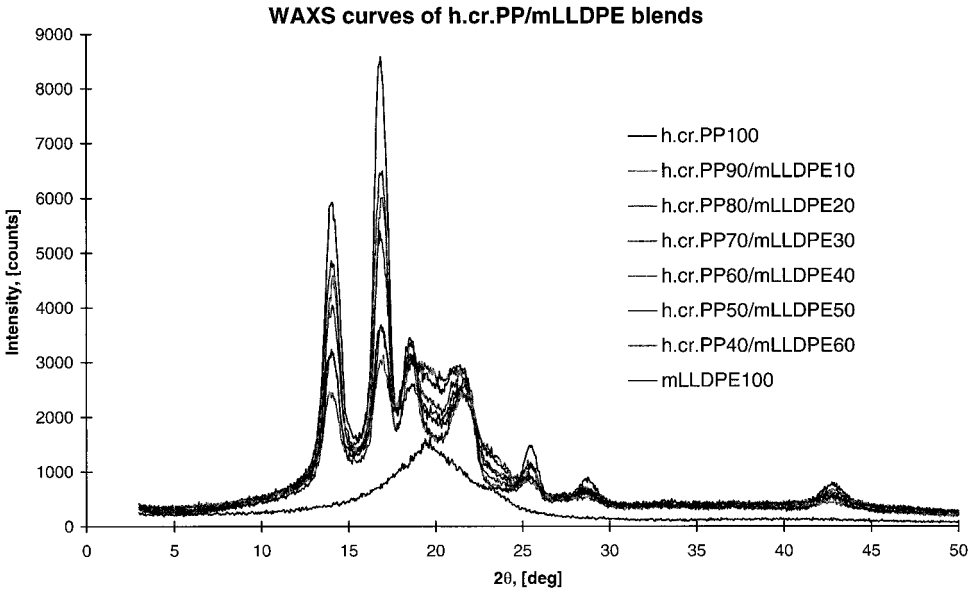

Figure 10 WAXS curves of h.cr.PP/mLLDPE blends.

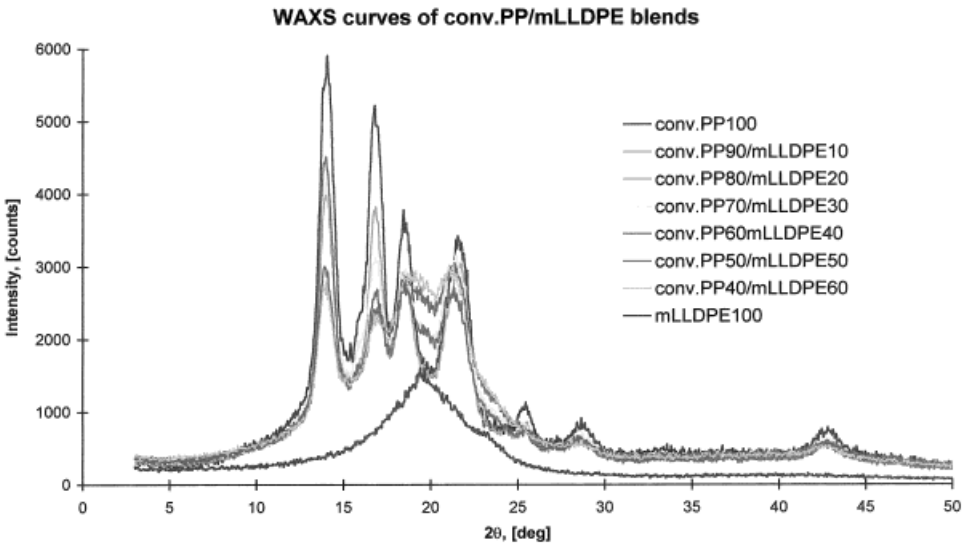

Figure 11 WAXS curves of conv.PP/mLLDPE blends.

conv.PP crystallize independently of the mLLDPE that is present. This confirms the data from MDSC tests, i.e., the level of crystallinity of PP in the blends did not depend on the composition.[1]

No new peaks are seen in the blends' curves. One change occurred in the blends of conv.PP with 10 and 20% mLLDPE: the small peak at 15.6°, corresponding to a β crystalline form of PP, became even smaller with an addition of mLLDPE. For the blends with 30% mLLDPE and higher, this peak became totally indistinguishable.

Overall, WAXS data confirmed that h.cr.PP/mLLDPE and conv.PP/mLLDPE blends are immiscible in the solid state. It seems likely that h.cr.PP contains some substances that suppresses the formation of the typical homogeneously disoriented spherulitic structure of isotactic PP.

CONCLUSIONS

1. In our previous study,[2] it was concluded that a co-continuous structure was responsible for the synergistic impact performance of the blends composed of conventional isotactic PP and mLLDPE. The current study on the h.cr.PP/mLLDPE blends confirmed the adequacy of this conclusion: it is found again that co-continuous type of structure has considerably improved toughness[1] compared with a dispersed-matrix structural type.
2. The correlation between the data from mechanical testing,[1] and the data from OM, MDSC,[1] and WAXS studies, shows that the stiffness, toughness, and thermal properties of PP may be advanced by altering its spherulitic nature, i.e., through suppression of the formation of spherulites.
3. The transformation of the conventional spherulitic structure seems to be performed through adding a very small amount of inorganic additives (nucleating agents), apparent in the very high T_{cr} of h.cr.PP, its higher absorption, and in a small additional peak at low angles on the WAXS curve.
4. A lamellar structure (particularly thickness of lamellae) in PP also influences its physical characteristics and properties of its blends. It might be possible that the fine lamellae observed in h.cr.PP in the present study is "a side effect" of the introduced nucleating agents.

N. Kukaleva gratefully acknowledges the financial support of Royal Melbourne Institute of Technology and Cooperative Research Centre for Polymers. The provision of research facilities (SEM, WAXS, and OM) by the Cooperative Research Centre for Polymers within the Department of Materials Science at Monash University is also truly appreciated.

REFERENCES

1. Kukaleva, N.; Cser, F.; Jollands, M.; Kosior, E. J Appl Polym Sci, to appear.
2. Kukaleva, N.; Jollands, M.; Cser, F.; Kosior, E. J Appl Polym Sci, to appear.
3. Coppola, F.; Greco, R.; Martuscelli, E.; Krammer, H. W.; Kummerlowe, C. Polymer 1987, 28, 47.
4. Chou, J.; Vijayan, K.; Kirby, D.; Hiltner, A.; Baer, E. J Mater Sci 1988, 23, 2521.
5. Bartczak, Z.; Galeski, A.; Martuscelli, E. Polym Eng Sci 1984, 24, 1155.
6. Lovinger, A. J.; Williams, M. L. J Appl Polym Sci 1980, 25, 1703.
7. Teh, J. W. J Appl Polym Sci 1983, 28, 605.
8. Kresge, E. N. J Appl Polym Sci Appl Polym Symp 1984, 39, 37.
9. Cser, F.; Rasoul, F.; Kosior, E. Polym Eng Sci 1999, 39, 1100.
10. Turner-Jones, A.; Aizlewood, J. M.; Beckett, D. R. Macromolecules 1964, 75, 134.
11. Tiganis, B. E.; Shanks, R. A.; Yu Long, J. Appl Polym Sci 1996, 59, 663.
12. Teh, J. W.; Rudin, A.; Keung, J. C. Adv Polym Technol 1994, 13, 1.
13. Xavier, S. F. In Two-Phase Polymer Systems; Utracki, L. A., Ed.; Hanser Gardner Publications: New York, 1991; Chapter 14.
14. Cullity, B. D. Elements of X-ray Diffraction; Addison-Wesley Publishing: London, 1978; Chapter 3.